Effect of Chemical Doping on the Electrical Conductivity of Poly(2,6-dimethyl-1,4-phenylene oxide)

A. K. KALKAR,[1,*] SHANKAR KUNDAGOL,[1] SURESH CHAND,[2] and SUBHAS CHANDRA[2]

[1]Centre of Advanced Studies in Applied Chemistry, Department of Chemical Technology, University of Bombay, Matunga, Bombay-400 019, India; and [2]National Physical Laboratory, New Delhi 110 012, India

SYNOPSIS

The electrical conductivity of solution-grown poly(2,6-dimethyl-1,4-phenylene oxide) (PPO) films doped with TCNQ, TCNE, TNF, and I_2 has been studied as a function of dopant concentration, temperature (298–353 K), and field (50–2000 V). PPO forms a conductive complex on doping with these strong electron-acceptor organic molecules. As with PPO, two distinct ohmic and nonohmic conduction regions at low and higher fields, respectively, are observed. The conduction properties of doped PPO films result from the formation of an isotropic continuous charge-transfer complex. The existence of such a complex is confirmed by UV-visible absorption spectra measurements. A possible mechanism for the electrical conduction process is discussed. © 1994 John Wiley & Sons, Inc.

INTRODUCTION

Considerable efforts have been devoted to the problems of changing the electrical conduction in polymers by intentional doping with typical low molecular weight organic compounds.[1-15] The charge carrier mobility can be greatly influenced by impregnating the polymer with suitable monomeric dopants. Depending on their chemical structure and the way in which they react with the macromolecular matrix, dopants influence the conductivity of the pristine polymers to different degrees.[5]

Poly(2,6-dimethyl-1,4-phenylene oxide) (PPO) is an important engineering plastic with many advantageous properties such as exceptionally high glass transition temperature (483 K), mechanical properties, flexibility, impact resistance, and stretchability. It is solution- and melt-processable. The pristine PPO, unlike a π-conjugated structure, has a low-order conductivity of 10^{-12} to 10^{-11} A.[16] However, due to its high potential for practical applications as a commercial thermoplastic, we have made an attempt to explore the possibilities of producing conductive PPO, in the semiconductor re-

gion, by charge-transfer interaction with different organic dopants.

In continuation of our early work[16] on electrical conduction in pristine PPO, the present article describes the effect of doping with highly electron acceptor molecules, 7,7,8,8-tetracyanoquinodimethane (TCNQ), tetracyanoethylene (TCNE), 2,4,7-trinitro-9-fluorenone (TNF), and iodine (I_2), on the charge carriers on PPO films.
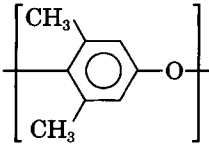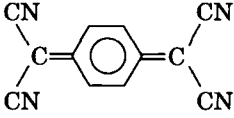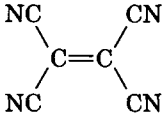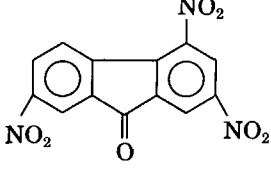
EXPERIMENTAL

Materials

The origin, purity, structure, and molecular weight of the different chemicals used in the present study are given in Table I. These chemicals were used without further purification. Spectroscopic-grade chloroform was used as a solvent and was obtained from either E. Merck, India, or S.D. Chemicals Ltd., India.

Film Preparation

Doped films were prepared by mixing different amounts of dopant in the nonsaturated solution of PPO in chloroform, followed by pouring the solution

---

Table I. The Monomer Structure Average Molecular Weight, Glass Transition Temperature, and Solubility of the Polymers Used and the Origin, Purity, Structure, Molecular Weight, and Melting Point of Dopants Used

Polymer	Monomer Structure	Average Molecular Weight	Glass Transition Temperature (%)	Solubility
PPO		1,000,000	484	Soluble in aromatic and chlorinated hydrocarbons

Dopant	Structure	Origin	Purity (%)	Molecular Weight	Melting Point (°C)
TCNQ		Fluka AG, Switzerland	98	204	290
TCNE		Aldrich Chemical Co. Inc., U.S.A.	98	128	198
TNF		Fluka AG, Switzerland	98	315	174
I_2	I—I	BDH Lab Chemicals Ltd., India	99.5	254	113

on a glass plate and allowing the solvent to evaporate. The PPO films having 0.25, 0.50, 0.75, and 1.0 wt % dopant concentration were prepared for all the dopants. The dopant concentration was calculated from the equation

$$\text{Dopant concentration (wt \%)} = \frac{W_d}{(W_p + W_d)} \times 100$$

where W_d and W_p represent the weight of dopant and the PPO, respectively. Thickness of the films, 70 mμ, was estimated using a micron gauge having an accuracy of ± 2 mμ. The details of the preparation of uniform and pinhole-free films have been reported earlier.[16]

Electrical Conductivity Measurements

The methods used for the preparation of a sandwich type of configuration (Al/PPO/Al) with aluminum electrodes on both sides of the film and the electrical conductivity measurements were the same as those reported earlier.[16] The steady static value of the current was recorded with a Keithley electrometer Model 610C.

Optical Absorption Studies

Ultraviolet (UV)-visible absorption spectra of pure PPO and doped PPO were recorded with a Pye-Unicam SP-8000 spectrophotometer in the solution phase using chloroform as solvent at room temperature.
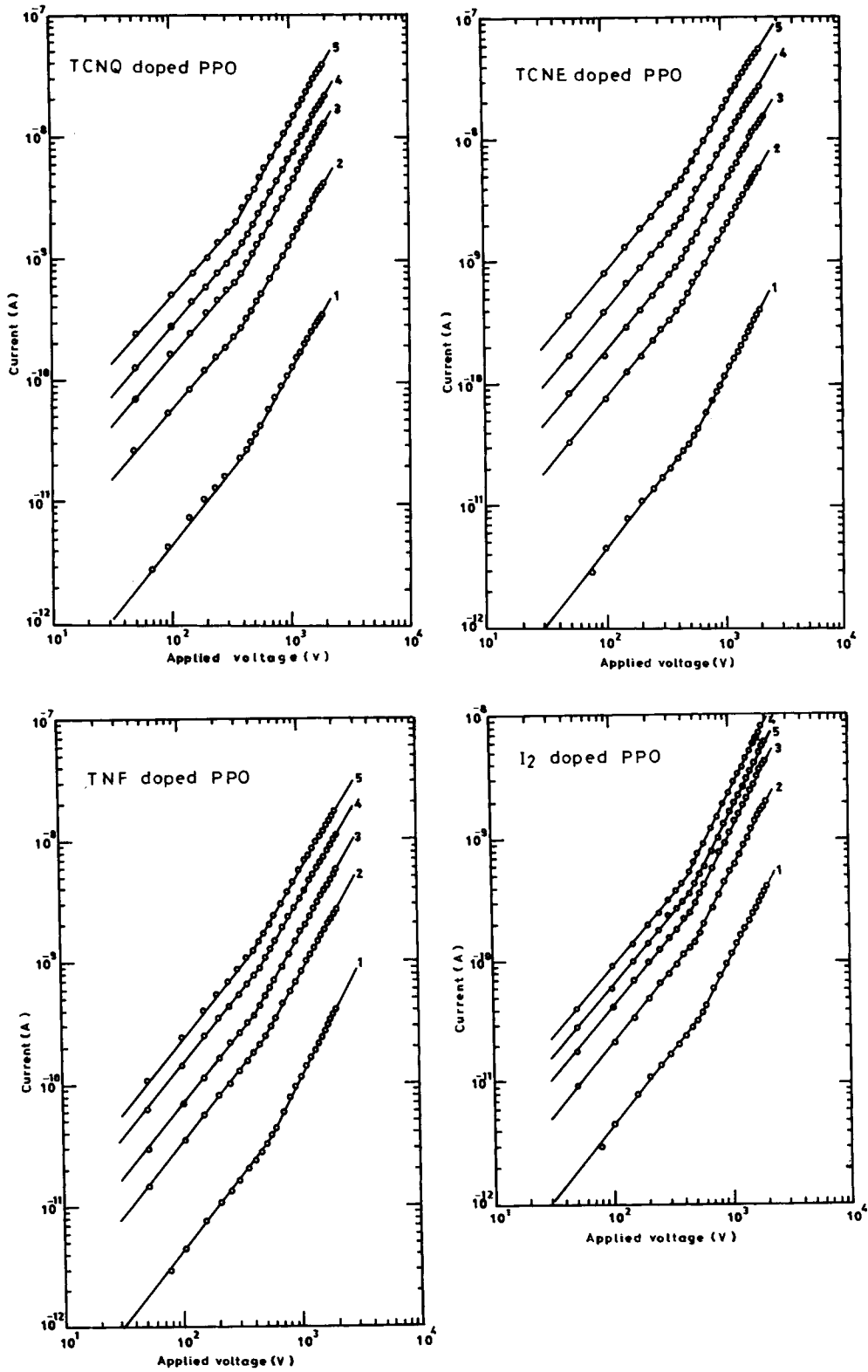
Figure 1 I–V characteristics of doped PPO films at 298K; curves 1–5 correspond to dopant concentrations of 0, 0.25, 0.50, 0.75, and 1.0 wt %, respectively.

Fourier transform infrared (FTIR) absorption spectra were obtained on a Bruker IFS-88 FTIR spectrophotometer. The thin films of pure PPO and doped PPO for spectral studies were cast from chloroform solutions on a NaCl window by the solution-evaporating technique at room temperature. This procedure facilitates obtaining equal thickness of undoped and doped PPO films. One hundred scans at a resolution of 2 cm^{-1} were signal-averaged.

Differential Thermal Analysis (DTA)

The glass transition temperatures of undoped and doped PPO films (15 mg) were obtained using a Stantan Redcroft Model STA-780 differential thermal analyzer. A heating cycle was made from room temperature to 600 K using a programmed heating rate of 5 K/min under nitrogen atmosphere. The values of the glass transition temperature were obtained by the intersection point of the projection of the base line with the tangent to the step.

Wide-angle X-ray Diffraction (WAXD)

The wide-angle X-ray scattering patterns of undoped and doped PPO films were performed at room temperature using a Phillips Model PW-1710 diffractometer and nickel-filtered CuKα radiation of wavelength 1.542 Å. The X-ray diffraction patterns were recorded from diffraction angles of $2\theta = 3°$ to $2\theta = 35°$ at a constant diffraction speed of 1°/min.

RESULTS AND DISCUSSION

The electrical current conduction in pristine and doped PPO films (70 mμ) were evaluated at a fixed temperature (298 K) but for different concentrations of TCNQ, TCNE, TNF, and I$_2$. The I–V characteristics for these doped films are shown in Figure 1. Curves 1–5 in these figures correspond to dopant concentrations of 0, 0.25, 0.50, 0.75, and 1.0 wt %, respectively. The general features of the I–V characteristics in doped films are the same as those of pure PPO.[16] The two similar distinct regions of conduction, which are an ohmic conduction with slope about 1 at low fields and a nonohmic conduction with slope about 2 at high fields, are invariably observed in all doped films. The variation of current for a bias of 100 V as a function of dopant concentration for all dopants is shown in Figure 2. It is observed that, as the dopant concentration increases, the current increases in the order of TCNE

$> \text{TCNQ} > \text{TNF} > \text{I}_2$. The saturation level was observed at 0.75 wt % of iodine, and a further increase in I$_2$ concentration leads to a decrease in current value. However, no saturation level was observed for other dopants up to the maximum concentration studied.

To obtain information on the effect of dopants on the activation energy of charge carriers responsible for the conduction, the current value at a fixed bias of 100 V for each film having different concentrations of the same dopants, viz., 0, 0.25, 0.50, 0.75, and 1.0 wt %, was monitored as a function of temperature. The Arrhenius plots of log I vs. $1/T$ for TCNQ, TCNE, TNF, and I$_2$ doped films are shown in Figure 3. These plots are straight lines and without break for the entire temperature range (298–353 K) studied. The activation energies were estimated for each case from the slopes of these curves using the relation

$$\sigma = \sigma_0 \cdot \exp(E/kT)$$

and are plotted against dopant concentrations (Fig. 4).

The activation energy decreases with increases in dopant concentration and is in the order of I$_2$ (0.73–0.64 eV) > TCNQ (0.71–0.53 eV) > TNF (0.68–0.52 eV) > TCNE (0.63–0.43 eV). However, in the case of I$_2$, it was observed to increase beyond
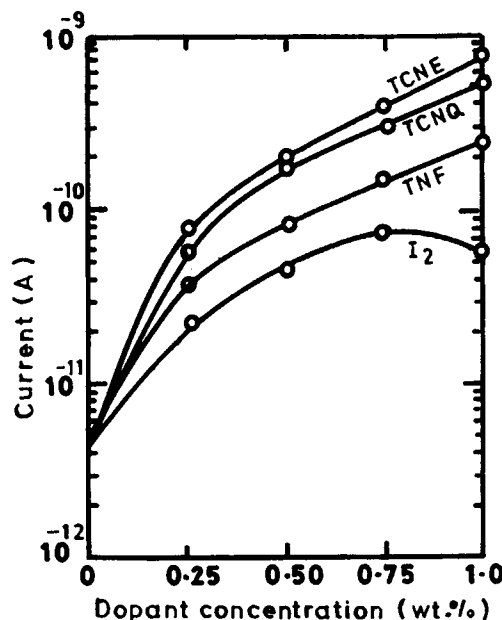

Figure 2   Plots of current for a bias of 100 V as a function of dopant concentration for PPO films.
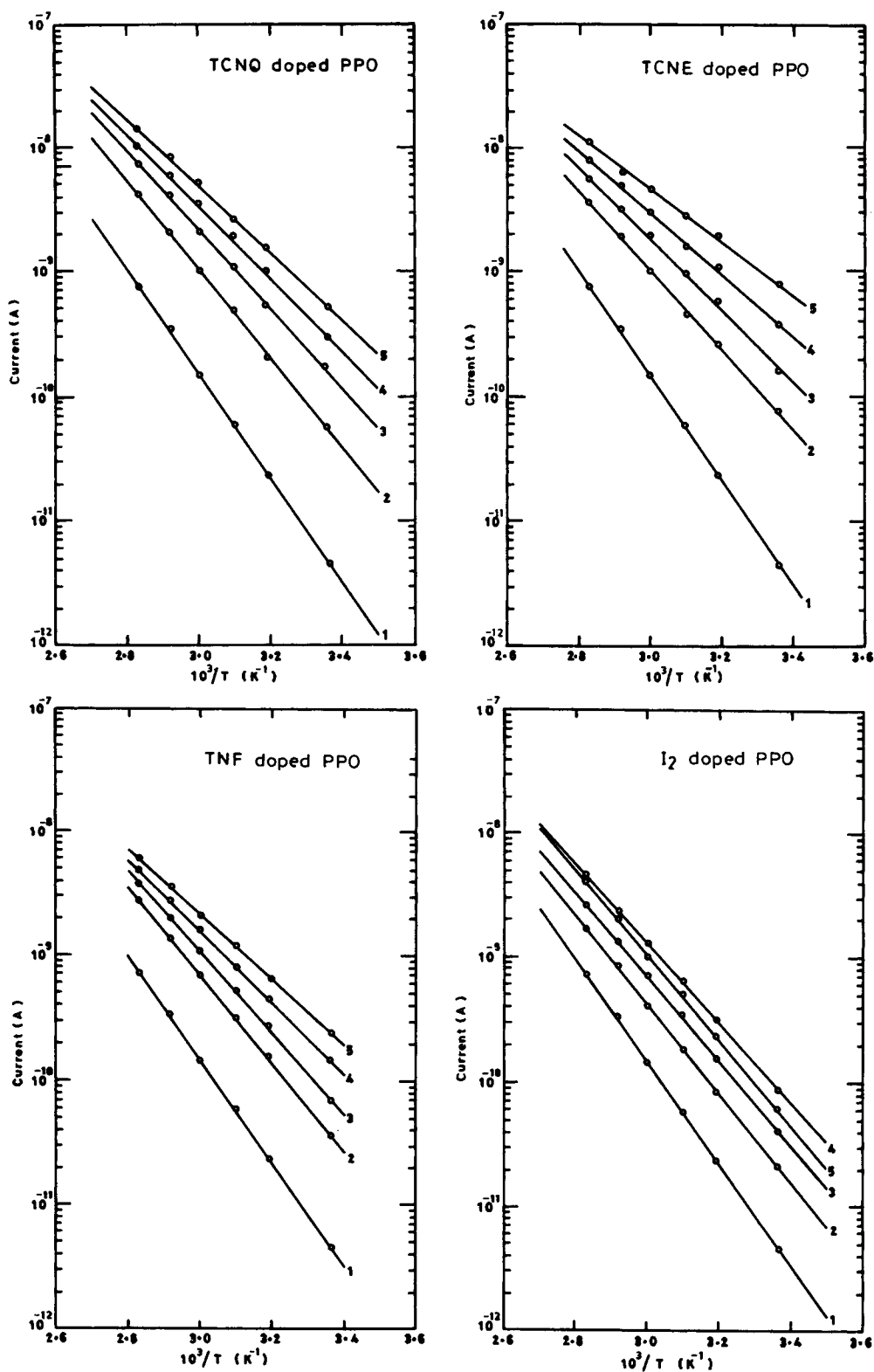
Figure 3   Log I vs. $1/T$ plots of doped PPO films at fixed bias voltage (100 V); curves 1–5 correspond to dopant concentrations of 0, 0.25, 0.50, 0.75, and 1.0 wt %, respectively.
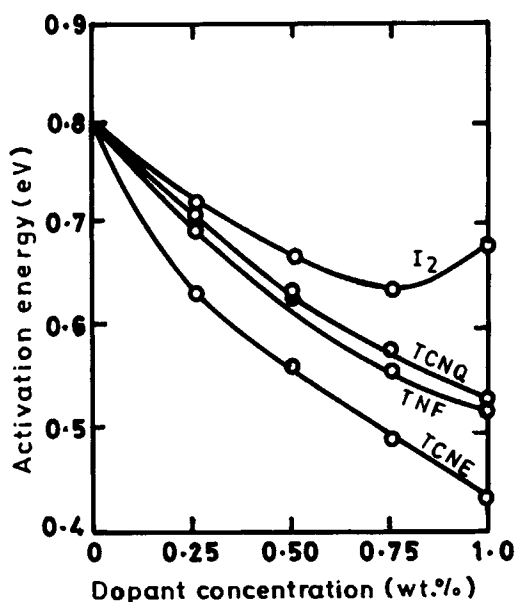
Figure 4   Plots of activation energy as a function of dopant concentration for PPO films.

Figure 6   Lowering of glass-transition temperature (T_g) of doped (1% wt concentration of dopant) PPO films; curves 1–5 correspond to pure PPO and TCNQ, TCNE, TNF, and I_2 doped PPO, respectively.

0.75 wt %. This may be attributed to the precipitation of iodine, which would result in a reduction in the free volume of the polymer and, hence, lead to steric hindrance to the movement of charge carriers.[8] In the undoped PPO, the activation energy was found to be 0.80 eV.[16] However, the charge transport in the iodine-doped PPO is via a charge-transfer state.

The mechanism of conduction in the doped PPO films can be understood by a detailed consideration of the formation of a PPO$^+$/dopant$^-$ charge transfer (CT) conducting complex. The formation of such a CT complex in the present case is evidenced in the
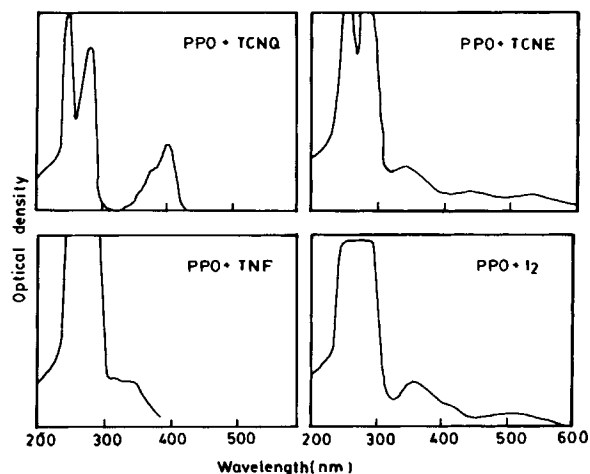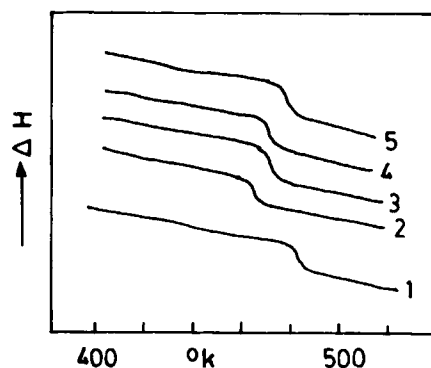
UV-visible absorption spectra by the appearance of the new low-energy absorption bands at 361 nm (I_2), 356 nm (TCNQ), 342 nm (TCNE), and 316 nm (TNF) in doped films. The fact that the absorption spectrum of PPO is changed by doping, as shown in Figure 5, indicates that all these dopants are effective and distributed homogeneously in PPO. Also, the lowering of the glass transition temperature of PPO after doping (Fig. 6) in DTA studies indicates that the dopants are acting as plasticizers. This, apart from the increased rate of diffusion of dopants, results in the more flexible doped PPO backbone that renders amorphous PPO more susceptible to interchain-dopant contact. Our WAXD studies (Fig. 7) reveal no crystallization in these doped films. The absence of crystalline peaks at $2\theta = 8°$, 13°, and 22° supports this conclusion.[17]

To understand the location of the sites of the defect centers produced by electronic doping in PPO chains (which eventually leads to an enhancement in the conduction), the FTIR absorption spectra of a 1 wt % of TCNE doped and undoped PPO films are compared in Figure 8. Similar spectral results have been observed for the other dopants. The frequencies of the $C\!=\!C$ stretching modes of the phenyl ring of the undoped PPO (1605, 1471, and 1381 cm^{-1}) shift to lower energy in the doped PPO (1585, 1457, and 1372 cm^{-1}). These phenyl ring modes appear to split into doublets. The band at 1021 cm^{-1} also exhibits splitting in the doped film spectrum and may be due to the ring bending mode. The phenyl oxygen cooperative stretch ($C\!-\!O\!-\!C$)[18] made at 1188 cm^{-1} shifts with a broader band profile to higher energy (1218 cm^{-1}). The frequencies of the $C\!-\!H$ stretching modes (3050–2850 cm^{-1}) are unaffected.

Figure 5   UV-visible absorption spectra of doped PPO.

These characteristic spectral features of doped PPO films are consistent with the lengthening of the C — C ring bonds and the shortening of the C — O bond due to the charge delocalization in doped PPO. The peak splitting of the C — C stretching modes suggests the doped region of the polymer chains, whereas the methyl substituents on phenyl rings are unaffected.

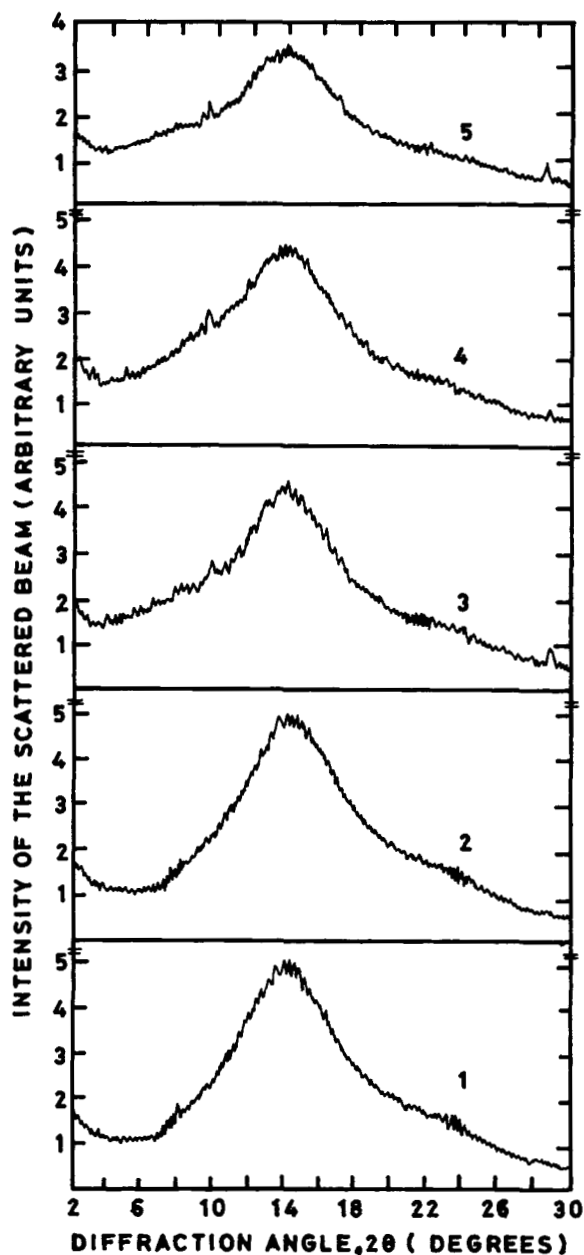Thus, in the present case, the various high-affinity

Figure 8   Infrared spectra of undoped PPO (curve A) and TCNE doped (1% wt concentration) PPO (curve B).

organic acceptors used as dopants (TCNQ, TCNE, TNF, and I_2) interact with the PPO backbone main chain by altering the molecular orbital arrangement through electron interaction. This electron interaction between the donor (PPO) and the dopant acceptor segments leads to formation of an excited CT state that successively undergoes a field-assisted ionization process via formation of the loose ion pairs and, subsequently, in dissociation into free charge carriers [19-21]:

$$(C_8H_8^+O - \bar{A}) \xrightarrow[\text{field}]{\text{Electric}} (C_8H_8^+O - \bar{A})^*$$

$$(C_8H_8^+O - \bar{A})^* \xrightarrow[\text{field}]{\text{Electric}} (C_8H_8^+O) + (\bar{A})$$

In the present case, as the strong electron affinity acceptors are used as dopants, the enhanced conductivity in doped PPO films thus may be attributed to the anions formed via electron transfer from the

Figure 7   X-ray diffraction pattern of undoped and doped PPO films; curves 1–5 correspond to pure PPO and 1% wt concentration of TCNQ, TCNE, TNF, and I_2, respectively.
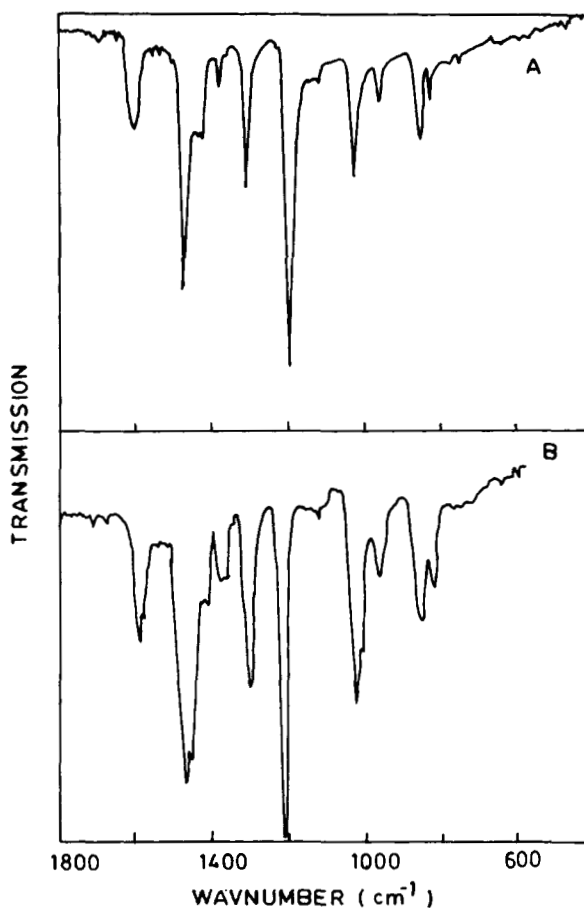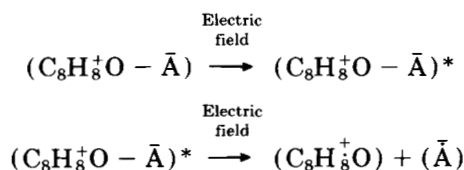
PPO to the acceptor dopant. The transport of the charge then occurs via anionic states.

REFERENCES

1. D. J. Sandman, *Mol. Cryst. Liq. Cryst.*, **50**, 235 (1979).
2. T. Tsutui, N. Nitta, and S. Saito, *Rep. Progr. Polym. Jpn.*, **24**, 216 (1981).
3. P. C. Mehendru, J. P. Agarwal, K. Jain, and A. V. R. Warrier, *Thin Solid Films*, **78**, 251 (1981).
4. L. W. Shacklette, R. L. Elsenbaumear, R. R. Chance, H. Eckhardt, J. E. Frommer, and R. H. Baughman, *J. Chem. Phys.*, **75**, 1919 (1982).
5. E. K. Sichel, M. Knowles, M. Rubner, and J. George, Jr., *Phys. Rev. B*, **25**, 5574 (1982).
6. L. Burda, A. Tracz, T. Pakula, J. Ulanski, and M. Kryszewski, *J. Phys. D. Appl. Phys.*, **16**, 1737 (1983).
7. J. E. Frommer, R. L. Elsenbaumer, H. Eckhardt, and R. R. Chance, *J. Polym. Sci. Poly. Lett. Ed.*, **21**, 39 (1983).
8. S. Chand, J. P. Agarwal, and P. C. Mehendru, *Thin Solid Films*, **109**, 109 (1983).
9. H. W. Gibson, *Polymer*, **25**, 3 (1984).
10. S. Tokito, T. Tsutui, and S. Saito, *Polym. J.*, **17**, 959 (1985).
11. S. Radhakrishnan and S. G. Joshi, *J. Micromol. Sci.*, **27**, 291 (1988).
12. N. C. Billinghan and P. D. Calvert, *Adv. Polym. Sci.*, **10**, 1 (1989).
13. S. Kanda and H. A. Phol, in *Organic Semiconducting Polymers*, J. E. Keton, Ed., Marcel Dekker, New York, 1968, p. 87.
14. R. L. Elsenbaumer and L. W. Shacklette, in *Handbook of Conducting Polymers*, T. A. Skothain, Ed., Marcel Dekker, New York, 1989, Vol. 1, p. 213.
15. J. Tanaka and M. Tanaka, in *Handbook of Conducting Polymers*, T. A. Skothain, Ed., Marcel Dekker, New York, 1989, Vol. 2, p. 1269.
16. A. K. Kalkar, S. Kundagol, S. Chand, and S. Chandra, *Thin Solid Films*, **196**, 361 (1991).
17. W. Wenig, R. Hammel, W. J. MacKnight, and F. E. Karasz, *Macromolecules*, **9**, 253 (1976).
18. M. M. Coleman and P. C. Painter, *Appl. Spectrosc. Rev.*, **20**, 255 (1984).
19. L. Onsager, *Phys. Rev.*, **54**, 558 (1938).
20. D. M. Pai and R. C. Enck, *Phys. Rev. B.*, **11**, 5163 (1975).
21. P. C. Mehendru, N. L. Pathak, K. Jain, and P. Mehendru, *Phys. Stat. Sol. (a)*, **42**, 403 (1972).